Analysis of MC-CDM and Cyclically Prefixed DS-CDM

Shinsuke Hara†, Yoshitaka Hara‡, and Shigehiko Tsumura†
† Graduate School of Engineering, Osaka University, Osaka, Japan
‡ Mitsubishi Electric Information Technology Centre Europe B.V. (ITE), Rennes, France

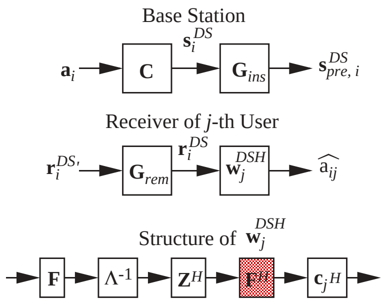

Fig. 1. Block diagram of a CP-DS-CDM scheme.

Abstract—**This paper theoretically analyzes the performance of Multi-Carrier Code Division Multiplexing (MC-CDM) and Cyclically Prefixed Direct-Sequence Code Division Multiplexing (CP-DS-CDM) in multipath fading channels. The paper shows the relationship among the SNIR, diversity order obtained and BER lower bound for MC-CDM and CP-DS-CDM, and demonstrates some computer simulation results on performance comparison.**

I. Introduction

Block transmission with cyclic prefix is a large class of transmission scheme including Orthogonal Frequency Division Multiplexing (OFDM)[1], Multicarrier-Code Division Multiplexing (MC-CDM)[2] and Direct Sequence-Code Division Multiplexing with cyclic prefix (called "cyclically prefixed (CP)-DS-CDM in this paper)[3], and it has drawn a lot of attention as a means to equalize the distortion/impairment experienced through a multipath fading channel in the frequency domain instead of in the time domain[4]. The mechanism for a chain of transmitter, a multipath fading channel and receiver is well theoretically analyzed in [5].

The references [6],[7] have discussed the pros and cons of MC-CDM and CP-DS-CDM theoretically and by computer simulation. This paper tries to theoretically show the relationship among the Signal to Noise pulse Interference Ratio (SNIR), diversity gain obtained and Bit Error Rate (BER) lower bound for the two schemes.

II. Analysis of CP-DS-CDM

A. CP-DS-CDM Scheme

Figure 1 shows the block diagram of a CP-DS-CDM scheme. Assume a case where a base station transmits data symbols to total J users (mobile terminals) using spreading codes with length of M over a multipath fading downlink channel. The ith signal is written in a vector form as $(M \times 1)$

$$\mathbf{s}_i^{DS} = \mathbf{C}\mathbf{a}_i. \tag{1}$$

In Eq.(1), $\mathbf{a}_i$ is the ith transmitted data symbol vector $(J \times 1)$, and $\mathbf{C} = [\mathbf{c}_1, \cdots, \mathbf{c}_j, \cdots, \mathbf{c}_J]$ is the spreading code matrix $(M \times J)$ ($\mathbf{c}_j$ is the spreading code vector $(M \times 1)$ of the jth user).

If the multipath fading channel has an impulse response with length of L, then the base station inserts a cyclic prefix with length of N $(N > L)$ to mitigate the inter-symbol interference introduced by the channel. The ith cyclically prefixed transmitted signal is written in a vector form as $((M+N) \times 1)$

$$\mathbf{s}_{pre,i}^{DS} = \mathbf{G}_{ins}\mathbf{s}_i^{DS}. \tag{2}$$

where $\mathbf{G}_{ins}$ is the cyclic prefix insertion matrix $((M+N) \times M)$[5]:

$$\mathbf{G}_{ins} = \begin{bmatrix} \mathbf{0}_{N\times(M-N)} \quad \mathbf{I}_{N\times N} \\ \mathbf{I}_{M\times M} \end{bmatrix} \tag{3}$$

where $\mathbf{0}$ is the matrix whose elements are all 0 and $\mathbf{I}$ is the identity matrix.

Through the multipath fading channel, the ith received signal contains a contribution from not only the ith transmitted signal but also the (i-1)th transmitted signal due to the multipath propagation, in addition to an additive white Gaussian noise. Therefore, it is written in a vector form as $((M+N) \times 1)$

$$\mathbf{r}_i^{DS\prime} = \mathbf{H}_{i,i}\mathbf{s}_{pre,i}^{DS} + \mathbf{H}_{i-1,i}\mathbf{s}_{pre,i-1}^{DS} + \mathbf{x}'_i \tag{4}$$

where $\mathbf{x}'_i$ is the noise vector $((M+N) \times 1)$, $\mathbf{H}_{i,i}$ and $\mathbf{H}_{i-1,i}$ are the ith channel impulse response matrices $((M+N) \times (M+N))$ contributed from the ith transmitted signal and the (i-1)th transmitted signal respectively.

The receiver first removes the cyclic prefix from the ith received signal:

$$\mathbf{r}_i^{DS} = \mathbf{G}_{rem}\mathbf{r}_i^{DS\prime} \tag{5}$$

where $\mathbf{G}_{rem}$ is the cyclic prefix removal matrix $(M \times (M+N))$:

$$\mathbf{G}_{rem} = [\mathbf{0}_{M\times N} \quad \mathbf{I}_{M\times M}]. \tag{6}$$

Taking into consideration $(L < N)$:$\mathbf{G}_{rem}\mathbf{H}_{i-1,i} = \mathbf{0}_{M\times(M+N)}$, (5) finally becomes

$$\mathbf{r}_i^{DS} = \mathbf{D}\mathbf{s}_i^{DS} + \mathbf{x}_i \tag{7}$$

where $\mathbf{r}_i^{DS}$ and $\mathbf{x}_i$ are the ith received signal vector $(M \times 1)$ and the noise vector $(M \times 1)$, respectively, and $\mathbf{D}$ is the channel distortion matrix $(M \times M)$:

$$\mathbf{D} = \mathbf{G}_{rem}\mathbf{H}_{i,i}\mathbf{G}_{ins}. \tag{8}$$

B. MMSE Combining

Consider the following minimization problem:

$$minimize \quad MSE(\mathbf{w}_j^{DS}) = E\left[|a_{ij} - \mathbf{w}_j^{DSH}\mathbf{r}_i^{DS}|^2\right] \quad (9)$$

where $E[(\cdot)]$ and H denote ensemble average and Hermitian transpose, respectively. The solution, namely, the minimum mean square error (MMSE) weight for the DS-CDM scheme, is given by[6]

$$\begin{aligned} \mathbf{w}_j^{DS} &= \mathbf{F}^H\mathbf{\Lambda}^{-1}\mathbf{Z}\mathbf{F}\mathbf{c}_j, & (10)\\ \mathbf{\Lambda}^{-1} &= diag\left\{\left(\frac{J}{M}|z_1|^2 + \sigma_{noise}^2\right)^{-1}, \cdots,\right. \\ &\qquad \left.\left(\frac{J}{M}|z_M|^2 + \sigma_{noise}^2\right)^{-1}\right\} & (11) \end{aligned}$$

where $\mathbf{F}$ is the M-point discrete Fourier transform (DFT) matrix ($M \times M$), the matrix $\mathbf{Z}$ is defined as

$$\mathbf{Z} = diag\{z_1, \cdots, z_M\} = diag\{\mathbf{Fh}\} \quad (12)$$

with the definition of the channel impulse response vector ($M \times 1$) as (T denotes transpose)

$$\mathbf{h} = [h_1, \cdots, h_L, h_{L+1}(=0), \cdots, h_N(=0)]^T \quad (13)$$

and σ_{noise}^2 is the power of noise.

C. SNIR

The signal to noise pulse interference power ratio (SNIR) is given by[8]

$$\begin{aligned} \mathrm{SNIR}^{DS} &= \frac{E\left[|\widehat{a_{ij}}|^2\right]}{E\left[|a_{ij}|^2\right] - E\left[|\widehat{a_{ij}}|^2\right]} \\ &= \frac{1}{1 - \sum_{m=1}^{M} \frac{|\widetilde{c_{mj}}|^2|z_m|^2}{\frac{J}{M}|z_m|^2+\sigma_{noise}^2}} - 1 \quad (14) \end{aligned}$$

where $\widetilde{c_{mj}}$ is the mth element of the discrete Fourier Transform of $\mathbf{c}_j$. If the spreading code is purely random, then it has a white (flat) power spectrum, so (14) can be written as

$$\mathrm{SNIR}^{DS} = \frac{1}{1 - \sum_{m=1}^{M} \frac{\frac{1}{M}|z_m|^2}{\frac{J}{M}|z_m|^2+\sigma_{noise}^2}} - 1. \quad (15)$$

D. BER Lower Bound

To analyze the BER lower bound, assume $J = 1$. In this case, the BER lower bound is given by[9]

$$BER_{lb}^{DS} \approx \begin{pmatrix} 2M_{eff} - 1 \\ M_{eff} \end{pmatrix} \frac{1}{\prod_{m=1}^{M_{eff}} (4\alpha_m/(M\sigma_{noise}^2))} \quad (16)$$

where $\alpha_1 \geq \alpha_2 \geq, \cdots, \geq \alpha_{M_{eff}} \geq 0$ are the eigenvalues of the auto-correlation matrix of $\mathbf{z}$:

$$\begin{aligned} \mathbf{z} &= [z_1, \cdots, z_M]^T & (17)\\ \mathbf{\Phi}_f &= E_{\mathbf{z}}\left[\mathbf{z}\mathbf{z}^H\right] = \{\phi_{t,u}\} & (18)\\ \phi_{t,u} &= \phi_{t,u}^* = E_z\left[z_t z_u^*\right] = \phi(\Delta = t-u) & (19) \end{aligned}$$

and M_{eff} denotes the effective diversity order.

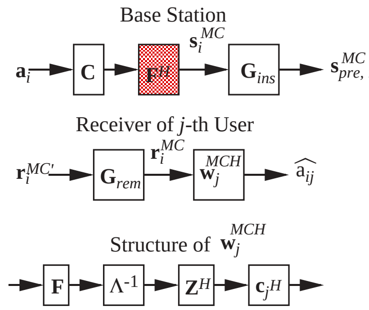

Fig. 2. Block diagram of MC-CDM scheme.

III. Analysis of MC-CDM

A. MC-CDM Scheme

Figure 2 shows the block diagram of an MC-CDM scheme. The MC-CDM scheme spreads the signal in the frequency domain, so using (1), the ith signal vector is written as

$$\mathbf{s}_i = \mathbf{s}_i^{MC} = \mathbf{F}^H\mathbf{s}_i^{DS} = \mathbf{F}^H\mathbf{C}\mathbf{a}_i. \quad (20)$$

B. MMSE Combining

The MMSE weight for the MC-CDM scheme is given by[6]

$$\mathbf{w}_j^{MC} = \mathbf{F}^H\mathbf{\Lambda}^{-1}\mathbf{Z}\mathbf{c}_j. \quad (21)$$

C. SNIR

The SNIR for the MC-CDM scheme is obtained as

$$\mathrm{SNIR}^{MC} = \frac{1}{1 - \sum_{m=1}^{M} \frac{\frac{1}{M}|z_m|^2}{\frac{J}{M}|z_m|^2+\sigma_{noise}^2}} - 1. \quad (22)$$

D. BER Lower Bound

The BER lower bound is given by

$$BER_{lb}^{MC} \approx \begin{pmatrix} 2M_{eff} - 1 \\ M_{eff} \end{pmatrix} \frac{1}{\prod_{m=1}^{M_{eff}} (4\alpha_m/(M\sigma_{noise}^2))}. \quad (23)$$

IV. Discussion on MC-CDM and CP-DS-CDM

A. Receiver Complexity

Comparing Fig.1 with Fig.2, it is clear that the receiver of the CP-DS-CDM scheme requires an additional inverse Fourier matrix $\mathbf{F}^H$ whereas it is moved to the base station for the MC-CDM scheme. Therefore, the receiver structure of MC-CDM is less complex than that of CP-DS-CDM.

B. Equivalence

(15) is equivalent to (22), so the BER performance of CP-DS-CDM is all the same as that of MC-CDM, as long as the same spreading gain and the same length of cyclic prefix are used in the two schemes and the length of DFT window in the MC-CDM scheme is the same as the length of block in the CP-DS-CDM scheme. Therefore, MC-CDM has no advantage over CP-DS-CDM in terms of attainable performance in multipath fading channels.

C. Relationship among SNIR, Diversity Order and BER Lower Bound

Assuming a full load case; $J = M$, (15) leads to

$$\begin{aligned} \mathrm{SNIR} &= \mathrm{SNIR}^{DS} = \mathrm{SNIR}^{MC} \\ &= \frac{1}{\frac{1}{M}\sum_{m=1}^{M} \frac{\sigma_{noise}^2}{|z_m|^2+\sigma_{noise}^2}} - 1. \end{aligned} \tag{24}$$

Using the following relationship:

$$\frac{1}{\frac{1}{M}\sum_{m=1}^{M}\frac{1}{y_m}} \leq \left(\prod_{m=1}^{M} y_m\right)^{\frac{1}{M}} \leq \frac{1}{M}\sum_{m=1}^{M} y_m \tag{25}$$

(24) leads to

$$\mathrm{SNIR} \leq \sum_{m=1}^{M} \frac{|z_m|^2}{M\sigma_{noise}^2}. \tag{26}$$

The equality holds if $z_1 = z_2 = \cdots = z_M$ (frequency non-selective fading). Therefore, the higher the correlations among the frequency responses become ($z_1 \approx z_2 \approx \cdots \approx z_M$), the higher the SNIR becomes, namely, the more the power of multiplexing interference can be reduced;

$$\begin{aligned} if\ \ |\phi_{t,u}^{high}| &\geq |\phi_{t,u}^{low}|\ (t \neq u), \\ then\ \ \mathrm{SNIR}^{high} &\geq \mathrm{SNIR}^{low} \end{aligned} \tag{27}$$

where the superscripts *high* and *low* denote the high and low correlation cases, respectively. However, even if the power of multiplexing interference can be more eliminated for the sake of higher correlations among the frequency responses, the BER lower bound becomes worse because of less effective diversity order (see the Appendix A);

$$\begin{aligned} if\ \ |\phi_{t,u}^{high}| &\geq |\phi_{t,u}^{low}|\ (t \neq u), \\ then\ \ BER_{lb}^{high} &\geq BER_{lb}^{low}. \end{aligned} \tag{28}$$

Consequently, there is a trade off between the reducible interference power and the attainable BER.

V. Analysis of Uncoded Subcarrier Blocked and Interleaved MC-CDM

A. Subcarrier Blocked and Interleaved MC-CDM Schemes

In recent discussion on practical MC-CDM schemes, the number of subcarriers is often different from the value of spreading gain. Figure 3 shows two types of MC-CDM schemes such as subcarrier blocked MC-CDM scheme[10] which maps a spread information over a subcarrier block and subcarrier interleaved MC-CDM scheme which maps a spread information over subcarriers with maximal separation. In both schemes, the input data sequence is first converted into Q parallel data sequences $(a_{i1j}, a_{i2j}, \cdots, a_{iQj})$ and each serial/parallel converter output is multiplied with the spreading code with length of K ($M = Q \times K$). To pay attention only to a parallelized data sequence ($q = 1, \cdots, Q$), define the qth parallelized symbol vector in the ith symbol interval as $(J \times 1)$

$$\mathbf{a}_{iq} = [a_{iq1}, \cdots, a_{iqj}, \cdots, a_{iqJ}]^T. \tag{29}$$

In addition, define the spreading code matrix $(K \times J)$ and the spreading code vector $(K \times 1)$ as

$$\begin{aligned} \mathbf{C} &= [\mathbf{c}_1, \cdots, \mathbf{c}_j, \cdots, \mathbf{c}_J] & (30) \\ \mathbf{c}_j &= [c_{1j}, \cdots, c_{kj}, \cdots, c_{Kj}]^T & (31) \\ |c_{kj}|^2 &= 1/K. & (32) \end{aligned}$$

With a mapping matrix $\mathbf{B}$ $(M \times K)$, the ith signal vector contributed only from the qth parallelized symbol is written as

$$\mathbf{s}_i = \mathbf{s}_{iq}^{MC} = \mathbf{F}^H \mathbf{B}_q \mathbf{C} \mathbf{a}_{iq}. \tag{33}$$

In (33), $\mathbf{B}_q$ can be written as

$$\mathbf{B}_q^{blk} = \begin{bmatrix} \mathbf{0}_{K\times K} \\ \vdots \\ \mathbf{0}_{K\times K} \\ \mathbf{I}_{K\times K} \\ \mathbf{0}_{K\times K} \\ \vdots \\ \mathbf{0}_{K\times K} \end{bmatrix} \begin{matrix} \left.\vphantom{\begin{matrix}a\\a\\a\end{matrix}}\right\} q-1 \\ \\ \left.\vphantom{\begin{matrix}a\\a\\a\end{matrix}}\right\} Q-q \end{matrix} \tag{34}$$

$$\mathbf{B}_q^{int} = \begin{bmatrix} & & \mathbf{0}_{(q-1)\times K} & & \\ 1 & 0 & \cdots & \cdots & 0 \\ & & \mathbf{0}_{Q\times K} & & \\ 0 & 1 & 0 & \cdots & 0 \\ & & \mathbf{0}_{Q\times K} & & \\ & & \vdots & & \\ 0 & \cdots & \cdots & 0 & 1 \\ & & \mathbf{0}_{(2Q-K-q+1)\times K} & & \end{bmatrix} \tag{35}$$

where the superscripts *blk* and *int* denotes subcarrier blocked and interleaved MC-CDM schemes, respectively.

B. MMSE Combining

Replacing $\mathbf{c}_j$ by $\mathbf{B}_q\mathbf{c}_j$ in (21) leads to

$$\mathbf{w}_{qj}^{MC} = \mathbf{F}^H \mathbf{\Lambda}^{-1} \mathbf{Z} \mathbf{B}_q \mathbf{c}_j. \tag{36}$$

C. SNIR

From (34) and (35), subcarrier blocking and interleaving change only the index for the subcarriers summed up in (22), so the SNIRs for the subcarrier blocked and subcarrier interleaved MC-CDM schemes are given by

$$\mathrm{SNIR} = \frac{1}{1 - \sum_{k=1}^{K} \frac{\frac{1}{K}|z_{\nu(k)}|^2}{\frac{J}{K}|z_{\nu(k)}|^2+\sigma_{noise}^2}} - 1 \tag{37}$$

where $\nu(k)$ is given by

$$\nu(k) = \begin{cases} \nu(k)^{blk} = (q-1)K + k & (blocked) \\ \nu(k)^{int} = q + Q(k-1) & (interleaved) \end{cases}. \tag{38}$$

D. BER Lower Bound

Defining the frequency response vectors as $(K \times 1)$

$$\mathbf{z}_q = [z_{(q-1)K+1}, \cdots, z_{(q-1)K+k}, \cdots, z_{qK}]^T \quad (39)$$

its auto-correlation matrices is written as

$$\mathbf{\Phi}_{f,q} = E_{\mathbf{z}}\left[\mathbf{z}_q \mathbf{z}_q^H\right] = \{\phi_{t,u}\} \quad (40)$$

where $\phi_{t,u}$ is a function of only the difference $\Delta = t - u$ and with (38):

$$\phi_{t,u} = \begin{cases} \phi_{t,u}^{blk} = \phi(\Delta = t-u) & (blocked) \\ \phi_{t,u}^{int} = \phi(\Delta = Q(t-u)) & (interleaved) \end{cases} . \quad (41)$$

Therefore, the BER lower bound is given by

$$BER_{lb} \approx \begin{pmatrix} 2K_{eff} - 1 \\ K_{eff} \end{pmatrix} \frac{1}{\prod_{k=1}^{K_{eff}} (4\alpha_k/(K\sigma_{noise}^2))} \quad (42)$$

where α_k is the eigenvalueof $\mathbf{\Phi}_{f,q}$, K_{eff} is its effective diversity orders.

E. Relationship among SNIR, Diversity Order and BER Lower Bound

It is quite natural to assume that the magnitude of $\phi(\Delta)$ is a monotonous decreasing function:

$$|\phi_{t,u}| \geq |\phi_{t',u'}| \; (\Delta = t - u \leq \Delta' = t' - u'). \quad (43)$$

From (41) and (43), the following properties are satisfied:

$$\begin{aligned} \phi_{t,t}^{blk} &= \phi_{t,t}^{int} \;\; (t = 1, \cdots, M) & (44) \\ |\phi_{t,u}^{blk}| &\geq |\phi_{t,u}^{int}| \;\; (t, u = 1, \cdots, M, \; t \neq u) & (45) \end{aligned}$$

therefore, from (27),

$$\text{SNIR}^{blk} \geq \text{SNIR}^{int} \quad (46)$$

and (see the Appendix B)

$$BER_{lb}^{blk\ uncoded} \geq BER_{lb}^{int\ uncoded}. \quad (47)$$

Consequently, it is concluded that, *for uncoded case,* subcarrier blocked MC-CDM can mitigate multiplexing interference for a heavier load condition, whereas it suffers from a worse BER performance for a lighter load condition due to less frequency diversity order, on the other hand, subcarrier interleaved MC-CDM can achieve a better BER performance for a lighter load condition due to more frequency diversity order, whereas it is rich in multiplexing interference for a heavier load condition.

VI. BER Lower Bound of Coded Subcarrier Blocked and Interleaved MC-CDM Schemes

Frequency diversity gain is obtained through channel encoding/decoding as well as spectrum spreading/despreading. For the case of $J = 1$, the estimated data symbol for a_{iq1} is approximated as

$$\widehat{a_{iq1}}' \approx z_{\xi(q)} a_{iq1} + \tilde{x}_i'' \quad (48)$$

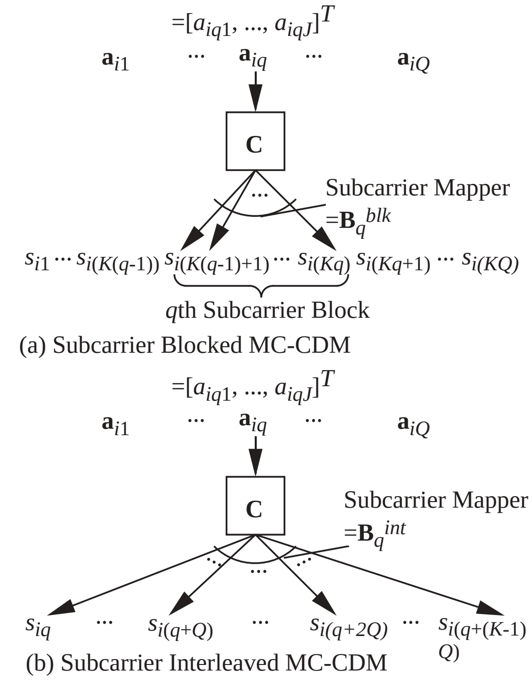

Fig. 3. Subcarrier blocked and interleaved MC-CDM.

where $\tilde{x}_i''$ is normalized to have the variance of σ_{noise}^2 and $\xi(q)$ is the median subcarrier index:

$$\begin{aligned} \xi(q)^{blk} &= \{(2q-1)K + 1\}/2 & (49) \\ \xi(q)^{int} &= \{2q + Q(K-1)\}/2. & (50) \end{aligned}$$

Defining the coefficient vector as $(Q \times 1)$

$$\kappa = [z_{\xi(1)}, \cdots, z_{\xi(Q)}]^T \quad (51)$$

its auto-correlation matix is written as

$$\begin{aligned} K &= E_\kappa\left[\kappa\kappa^H\right] = \{\psi_{t,u}\} & (52) \\ \psi_{t,u} &= E_z\left[z_{\xi(t)} z_{\xi(t)}^H\right]. & (53) \end{aligned}$$

From (49) and (50),

$$\begin{aligned} \psi_{t,t}^{int} &= \psi_{t,t}^{blk} \;\; (t = 1, \cdots, M) & (54) \\ |\psi_{t,u}^{int}| &\geq |\psi_{t,u}^{blk}| \;\; (t, u = 1, \cdots, M, \; t \neq u) & (55) \end{aligned}$$

consequently, similar to the discussion through (43) to (47),

$$BER_{lb}^{int\ coded} \geq BER_{lb}^{blk\ coded}. \quad (56)$$

Consequently, it is concluded that, *for coded case,* subcarrier blocked MC-CDM can mitigate multiplexing interference and can achieve a better BER performance due to frequency diversity order through coding.

VII. Numerical Results and Discussions

To confirm the theoretical results, computer simulation is carried out. A multipath delay profile with 18 exponentially decaying paths is assumed with no temporal variation of the channel. As a transmission system, the lengths of cyclic prefix and DFT window are 128 and 512, respectively, the processing gain is 32, the modulation is based on QPSK, and a half-rate turbo coding is assumed. The packet error rate (PER) is evaluated for a signal packet composed of 512 QPSK symbols.

Figures 4 and 5 show the PER against the average E_b/N_0 for fading channels with low and high frequency selectivity, respectively. Here, the RMS delay spread is normalized by the cyclic prefix length. When the frequency selectivity is low, for the lighter load conditions, the performance of the subcarrier interleaved MC-CDM and CP-DS-CDM schemes is better than that of subcarrier blocked MC-CDM scheme, because they can mitigate well the multiplexing interference and obtain the optimized frequency diversity gain. However, for the full load case, the performance of the subcarrier blocked MC-CDM scheme is better than that of subcarrier interleaved MC-CDM and CP-DS-CDM schemes, because it can suppress the multiplexing interference more and obtain a frequency diversity gain comparable to them. On the other hand, when the frequency selectivity is high, there are no large difference in PER among the three schemes. For the full load case, the performance of the subcarrier blocked MC-CDM scheme is slightly better than that of the other two schemes.

Figures 6 and 7 show the PER against the normalized RMS delay spread and the PER against the number of users. As long as the number and strength of the paths remain the same in the delay profiles, even if the frequency selectivity changes, the same PER should be achieved. In the both figures, the performance of the CP-DS-CDM and subcarrier interleaved MC-CDM schemes is insensitive to the value of the delay spread, on the other hand, the performance of the subcarrier blocked MC-CDM scheme is sensitive to the value of the delay spread. This is because the frequency diversity gain is optimally obtained through the MMSE criterion-based combining for the CP-DS-CDM and subcarrier interleaved MC-CDM schemes, whereas it is obtained through channel coding for the subcarrier blocked MC-CDM scheme, which is no longer optimal.

Finally, against the prediction by (56), when the number of users is one, the performance of the subcarrier blocked MC-CDM scheme does not outperform that of the CP-DS-CDM and subcarrier interleaved MC-CDM schemes. Especially, for the case of low frequency selectivity, it is much worse. This is because the frequency diversity gain obtained through channel coding is much smaller than that based on the optimal MMSE criterion-based combining.

VIII. Conclusions

This paper has theoretically shown the relationship among the SNIR, diversity order obtained and BER lower bound for MC-CDM and CP-DS-CDM. Furthermore, the paper has discussed their packet error rate in multipath fading channels by the computer simulation. Subcarrier blocked MC-CDM, which tries to obtain frequency diversity gain through channel coding and suppress multiplexing interference by blocked subcarrier mapping, is advantageous only for full load case.

Appendix A

Defining the auto-correlation matrix of the channel impulse response vector as

$$\mathbf{\Phi}_t = E_{\mathbf{h}}\left[\mathbf{h}\mathbf{h}^H\right]. \tag{57}$$

(57) can be also written as

$$\mathbf{\Phi}_f = \mathbf{F}\mathbf{\Phi}_t\mathbf{F}^H. \tag{58}$$

The rank and eigenvalues of a matrix is invariant through any linear transformations, so the rank of $\mathbf{\Phi}_f$ is L:

$$M_{eff} = L. \tag{59}$$

The length of the channel impulse response for higher correlations among the frequency responses must be shorter than that for lower correlations:

$$M_{eff}^{high} = L^{high} \leq L^{low} = M_{eff}^{low}. \tag{60}$$

Therefore,

$$\begin{aligned} BER_{lb}^{high} &\approx \begin{pmatrix} 2M_{eff}^{high}-1 \\ M_{eff}^{high} \end{pmatrix} \frac{1}{\prod_{m=1}^{M_{eff}^{high}}(4\alpha_m^{high}/\sigma_{noise}^2)} \\ &\geq \begin{pmatrix} 2M_{eff}^{low}-1 \\ M_{eff}^{low} \end{pmatrix} \frac{1}{\prod_{m=1}^{M_{eff}^{low}}(4\alpha_m^{low}/\sigma_{noise}^2)} \\ &\approx BER_{lb}^{low}. \end{aligned} \tag{61}$$

Appendix B

In general, the following properties are satisfied:[11]

$$\sum_{t=1}^{K}\alpha_t = trace\{\mathbf{\Phi}\} = \sum_{t=1}^{K}\phi_{t,t} \tag{62}$$

$$\sum_{t=1}^{M}\alpha_t^2 = \|\mathbf{\Phi}\|_F^2 = \sum_{t=1}^{M}\sum_{u=1}^{M}|\phi_{t,u}|^2 \tag{63}$$

where $trace\{(\cdot)\}$ and $\|(\cdot)\|_F$ denote the trace and Frobenius norm of $(\cdot)$. From (55), (55), (62) and (63), the eigenvalues α_t^{blk} and α_t^{int} (including 0) satisfy the following properties:

$$\sum_{t=1}^{K}\alpha_t^{blk} = \sum_{t=1}^{K}\alpha_t^{int} \tag{64}$$

$$\sum_{t=1}^{K}\alpha_t^{blk\,2} \geq \sum_{t=1}^{K}\alpha_t^{int\,2}. \tag{65}$$

$K\times$(65)-(64)$\times$(64) leads to

$$\sum_{t=1}^{K}\sum_{u=1}^{K}\left(\alpha_t^{blk}-\alpha_u^{blk}\right)^2 \geq \sum_{t=1}^{K}\sum_{u=1}^{K}\left(\alpha_t^{int}-\alpha_u^{int}\right)^2. \tag{66}$$

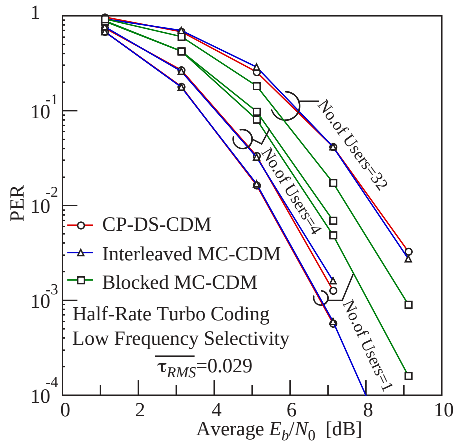

Fig. 4. PER for a low frequency selective channel.

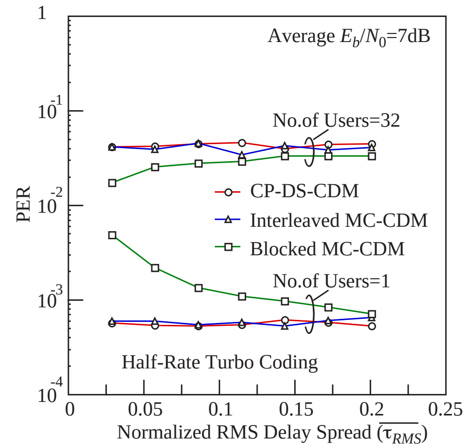

Fig. 6. PER against the RMS delay spread.

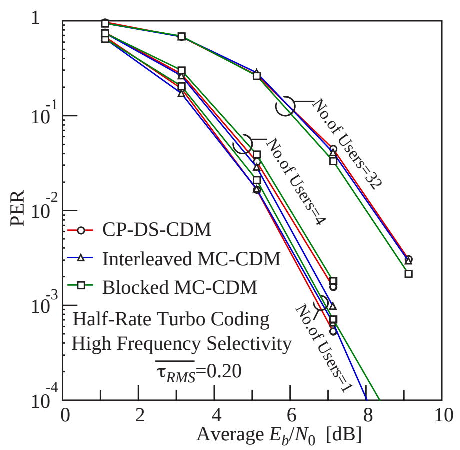

Fig. 5. PER for a highly frequency selective channel.

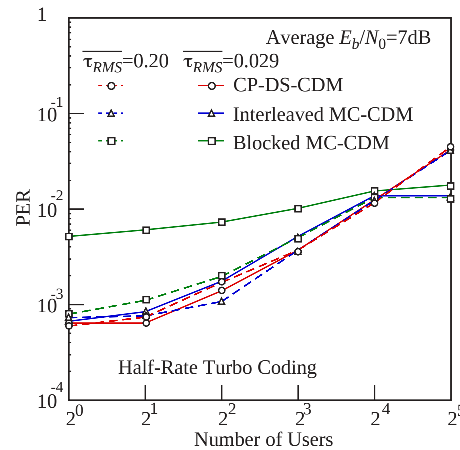

Fig. 7. PER against the number of users.

(66) means that the sum of the errors between any pairs of the eigenvalues for the subcarrier blocked MC-CDM scheme is greater than that for the subcarrier interleaved MC-CDM scheme. Define the average value of the eigenvalues as λ_{ave} and furthermore the number of eigenvalues which is far less than λ_{ave} as M'. (66) implies that

$$M'^{blk} \geq M'^{int}. \tag{67}$$

Note that the lowest eigenvalue $\lambda_{M_{eff}}$ should be reasonably large[9]. Therefore,

$$M_{eff}{}^{int} = M - M'^{int} \geq M_{eff}{}^{blk} = M - M'^{blk}. \tag{68}$$

and consequently,

$$BER_{lb}^{blk} \geq BER_{lb}^{int}. \tag{69}$$

References

[1] S. Hara and R. Prasad, *Multicarrier Techniques for 4G Mobile Communications,* Artech House Publishers, 2003.

[2] S. Hara and R. Prasad, "Overview of multicarrier CDMA," *IEEE Commun. Mag.,* vol. 35, no. 12, pp.126-144, Dec. 1997.

[3] S. Itagaki, T. Sao and F. Adachi, "Frequency and space diversity for orthogonal multicode DS-CDMA (in Japanese)," *Technical Report of IEICE,* RCS2002-341, pp.217-2221, Mar. 2002.

[4] D. Falconer, S. Ariyavisitakul, A. Benyamin-Seeyar and B. Eidson, "Frequency domain equalization for single-carrier broadband wireless system," *IEEE Commun. Mag.,* vol. 40, no. 12, pp.58-66, Apr. 2002.

[5] T. Kojima, K. Hayashi and H. Sakai, "A study on adaptive antenna array for single carrier modulation with cyclic prefix (in Japanese)," *Technical Report of IEICE,* RCS2002-339, pp.205-210, Mar. 2002.

[6] S. Hara, Y. Hara and S. Tsumura, "Can MC-CDM Outperform DS-CDM?," *Proc. APWCS,* pp.68-72, Jan. 2004.

[7] D. Garg and F. Adachi "Comparison of Chip Interleaved MC-CDMA and DS-CDMA with Frequency-domain Equalization," *Proc. APWCS,* pp.156-159, Jan. 2004.

[8] S. Haykin, *Adaptive Filter Theory,* 3rd ed., pp.194-240, Upper Saddle River: NJ, Prentice-Hall, 1996.

[9] M. Schwartz, W. R. Bennett and S. Stein, *Communication Sytems and Techniques,* pp.416-489, Piscataway: NJ, IEEE PRESS, 1996.

[10] H. Atarashi and M. Sawahashi, "Variable spreading factor orthogonal frequency and code division multiplexing (VSF-OFCDM)," *Proc. MC-SS2001,* pp.113-122, Sept. 2001.

[11] T. Kailath, A. H. Sayed and B. Hassibi, *Linear Estimation,* pp.725-742, Upper Saddle River: NJ, Prentice-Hall, 2000.